Recombination lifetimes in InN films studied by time-resolved excitation-correlation spectroscopy

Horng-Chang Liu, Chia-He Hsu, Wu-Ching Chou, Wei-Kuo Chen, and Wen-Hao Chang*
Department of Electrophysics, National Chiao Tung University, Hsinchu 300, Taiwan
(Received 13 August 2009; revised manuscript received 6 October 2009; published 10 November 2009)

Recombination dynamics in degenerate InN were investigated by means of time-resolved excitation-correlation spectroscopy. The photoluminescence decay times are determined beyond the spectral response and temporal resolution limits of conventional photon-counting detectors. Spectral and temperature dependence of decay times reveal the effects of hole localizations on the recombination mechanisms. At low temperatures, the radiative lifetime τ_r is insensitive to temperature and significantly longer than that predicted for the radiative band-to-band recombination, indicative of a transition dominated by the free-to-bound recombination without k conservation. Above a certain temperature determined by the electron concentration, we find $\tau_r \sim T^{3/2}$, as expected for the band-to-band transition when the k-selection rule holds. We determine a lower limit for the bimolecular recombination coefficient B in InN at 300 K as 5.6×10^{-11} cm^3/s.

DOI: 10.1103/PhysRevB.80.193203 PACS number(s): 78.20.−e, 78.47.Cd, 78.55.−m

Information about the recombination dynamics and carrier lifetimes in InN are indispensable for the development of near-infrared group III-nitride devices.[1] In principle, the recombination lifetimes can be obtained by time-resolved photoluminescence (TRPL) measurements using either a streak camera or a fast photomultiplier tube (PMT) to record PL decays. However, for high-quality InN with typical emission wavelengths in the range of 1.7–1.9 μm, the reported TRPL data are quite limited[2,3] because the photon-counting-based technique is problematic in this spectral range due to the lack of suitable photocathodes for wavelength longer than 1.7 μm.[4] Accordingly, some studies have turned to employee more sophisticated techniques, such as PL up conversion[5,6] and pump-probe differential transmission,[7,8] to measure the carrier lifetimes in InN.

Excitation-correlation (EC) spectroscopy is a convenient alternative to the conventional TRPL technique for the study of carrier lifetimes in semiconductor materials.[9–13] This technique, also known as picosecond or femtosecond EC, is based on the nonlinear dependence of PL intensity on the excitation intensity of two laser pulses with a relative time delay. By varying the delay time, the resulting time-resolved EC (TREC) trace can be used to determine carrier lifetimes. This technique is much easier to implement than the up-conversion technique but in principle yields the same temporal resolution limited only by the laser-pulse duration. In addition, this technique is applicable to the spectral range beyond 1.7 μm, which is particularly useful for the study of InN.

In this work, we investigated the recombination dynamics of n-type degenerate InN with different electron concentrations by using the TREC technique. The PL decay time in InN were determined. We have also performed temperature-dependent measurements to extract contributions of radiative and nonradiative lifetimes. We present here a detailed study on the influence of the carrier concentration on the hole localization in the valence-band (VB) tails as well as on the radiative recombination mechanisms in InN.

The sample investigated is a 300 nm InN film grown on an 1 μm GaN template on sapphire (0001) by metalorganic chemical vapor deposition. The detailed growth conditions can be found elsewhere.[14–16] Room-temperature Hall measurements of the sample showed a background electron concentration of 1.2×10^{19} cm^{-3}. A sample with a lower electron concentration was obtained by rapid thermal annealing at 650 °C in a N_2 environment for 30 s. In the annealed InN film, the Hall concentration is reduced to 3×10^{18} cm^{-3}. In EC measurements, a mode-locked Ti:sapphire laser delivering ~150-fs laser pulses (780 nm/80 MHz) was used as an excitation source. The laser beam was split into two beams of equal intensity to excite the sample. The two beams, with a relative interpulse time delay γ controlled by a 80-cm mechanical stage, were modulated at different frequencies (f_1 and f_2) and focused onto the same spot on the sample. The resulting PL signal was collected into a 0.5 m monochromator and detected by a liquid-nitrogen-cooled extended InGaAs photodiode with a cutoff wavelength at 2.1 μm. The EC signal was extracted from the sum-frequency component (f_1+f_2) by using a lock-in amplifier. For a comparison purpose, we have also measured TRPL by using a fast InGaAs PMT. The decay traces were recorded using the time-correlated single-photon-counting technique with an overall time resolution ~150 ps in the spectral range of 0.9–1.65 μm.

Figure 1(a) shows the time-integrated PL spectra for the as-grown and annealed InN samples measured at $T=12$ K under an excitation power of $P_{ex}=5$ mW. The PL emission band of InN can be characterized as *free-to-bound* recombination between the degenerate electrons in the conduction band and the photogenerated holes at the VB edge,[17,18] as schematically shown in Fig. 1(b). The PL peak energy for the annealed InN film is lower than the as-grown sample by ~70 meV, due to its lower electron concentration and hence a smaller Burstein-Moss shift. The corresponding EC spectra measured without interpulse delay (i.e., $\gamma=0$) are displayed in Fig. 1(c). For the as-grown sample, the EC signal shows a line shape almost the same as its PL spectrum, but with a negative intensity, except a weak positive feature emerging from the high energy side. By contrast, the EC spectrum for the annealed sample consists of both negative and positive signals on the low and high energy sides, respectively.

The EC signal, $S_{EC}(\hbar\omega,\gamma)$, detected at a given photon energy $\hbar\omega$, is a result of the nonlinear change in PL intensity due to excitations by the two laser pulses with an interpulse

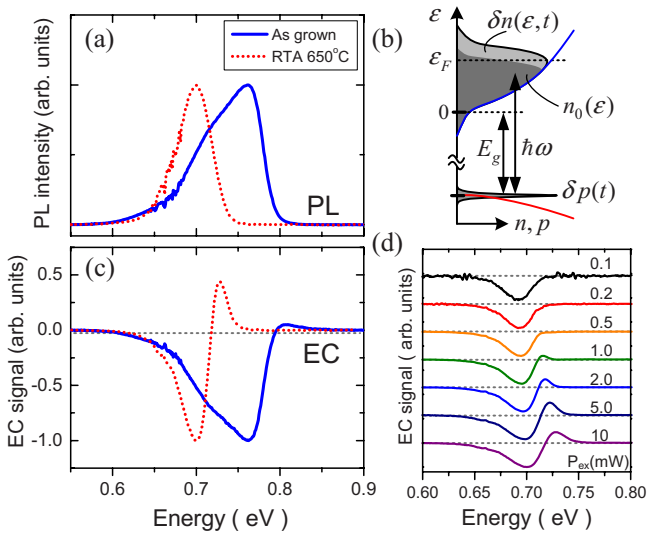

FIG. 1. (Color online) (a) The PL spectra for the investigated InN films measured at $T=12$ K. (b) A schematic diagram for the recombination paths in degenerate InN. (c) The EC spectra taken at zero delay for both samples under an excitation power of $P_{ex}=5$ mW. (d) The EC spectra for the annealed InN film under different excitation powers $P_{ex}=0.1-10$ mW. All the spectra have been normalized.

delay time γ. It can be written as[13] $S_{\mathrm{EC}}(\hbar\omega,\gamma)=I_{\mathrm{PL}}^{(2)}(\hbar\omega,\gamma)-2I_{\mathrm{PL}}^{(1)}(\hbar\omega)$, where $I_{\mathrm{PL}}^{(1)}$ and $I_{\mathrm{PL}}^{(2)}$ are the time-integrated PL intensity excited by one of the two beams and by both beams, respectively. For a n-type material with an electron concentration n_0, the EC signal is given by

$$S_{\mathrm{EC}}(\epsilon,\gamma)\propto\frac{1}{T}\int_0^T n_0(\epsilon)[\delta p_2(t,\gamma)-\delta p_1(t)]dt + \frac{1}{T}\int_0^T[\delta n_1(\epsilon,t)\delta p_2(t,\gamma)+\delta n_2(\epsilon,t,\gamma)\delta p_1(t)]dt, \quad (1)$$

where T is the laser period, $\epsilon\equiv\hbar\omega-E_g$, where E_g is the energy band gap, $n_0(\epsilon)$ is the energy distribution of the degenerate electron, and $\delta n_i(\delta p_i)$ with $i=1,2$ are the photogenerated electron (hole) concentrations by the first pulse at $t=0$ and the second pulse at $t=\gamma$, respectively. Here, we assume that the photogenerated holes are at the VB edge with a delta-function-like energy distribution so that the measured PL band corresponds to the energy distribution of degenerated electrons $n_0(\epsilon)$ in the conduction band.[16,17] From Eq. (1), it is obvious that two major effects will contribute to EC signals. The first one is the differential absorption arising from state filling. The photocarriers generated by the first pulse make the second pulse less likely to excite as many photocarriers due to fewer available states. Therefore, the first integral in Eq. (1) contributes a negative EC signal because $\delta p_2(t,\gamma)<\delta p_1(t)$. The second effect, i.e., the second integral in Eq. (1), is the cross recombination of the electrons δn_1 (holes δp_1) generated by the first pulse with holes δp_2 (electrons δn_2) by the second pulse. Because the second integral in Eq. (1) is always positive, the cross recombination

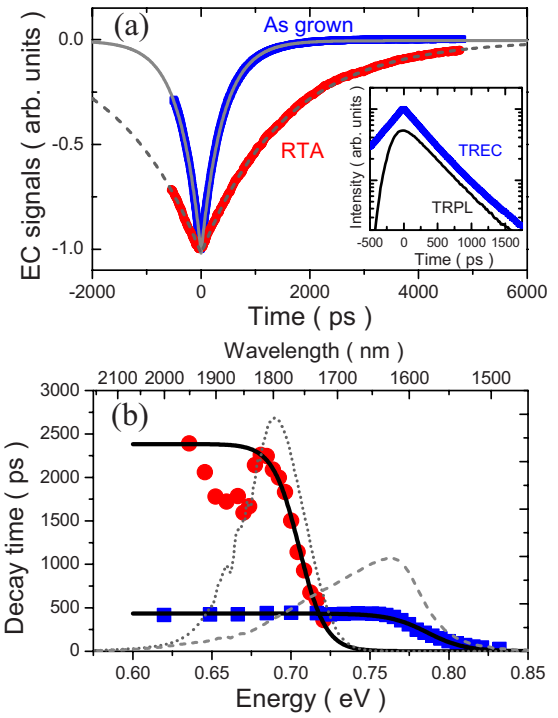

FIG. 2. (Color online) (a) TREC traces recorded at the energy of EC dips. The excitation power used is 5 mW (1 mW) for the as-grown (annealed) sample. Solid and dotted lines are single-exponential fits. The inset shows a comparison between the TRPL and the $|S_{\mathrm{EC}}(\gamma)|$ traces for the as-grown sample. (b) Spectral dependence of measured decay times $\tau(E)$ together with the corresponding PL spectra (dashed and dotted lines) for both samples. Solid lines are fitting curves.

will contribute a positive EC signal. In addition, since the photogenerated electrons $\delta n(\epsilon)$ were distributed near or above the Fermi energy ϵ_F, the positive EC signal occurs only on the high energy side of the PL band. It should be noted that the positive EC signal is significant only when δn is comparable to n_0. Due to the high electron concentration in the as-grown sample, the positive EC signal is not pronounced under excitation conditions used in this study. Conversely, as shown in Fig. 1(d), the positive EC signals for the annealed InN film can be observed when $P_{ex}\gtrsim 1$ mW, corresponding to a photogenerated carrier density of about $\delta n\sim 1.2\times 10^{17}$ cm^{-3} Ref. 19, which is noneligible as comparable with the background n_0.

The TREC traces for both samples recorded at the energy of EC dips as function of the delay time γ are shown in Fig. 2(a). Since the two beams are equal in intensity, the measured TREC traces are expected to be symmetric around $\gamma=0$. The data can be well described by a single-exponential function $Ae^{-|\gamma|/\tau}$, yielding a decay time constant τ. For n-type degenerate semiconductors under low excitation conditions, the cross recombination terms in Eq. (1) are negligible. If both δp_1 and δp_2 decay exponentially with a time constant τ_p, it can be shown from Eq. (1) that

$$S_{\mathrm{EC}}(\epsilon,\gamma)\propto n_0(\epsilon)(\delta p_2^0-\delta p_1^0)\tau_p e^{-\gamma/\tau_p}, \quad (2)$$

where δp_i^0 is the initial hole population created by the ith pulse. Therefore, the measured decay time τ from TREC

traces represents the minority-carrier lifetimes τ_p. Because the PL decay is also determined by the minority-carrier lifetime τ_p, i.e., $I_{\mathrm{PL}}(t) \propto n_0 \delta p(t)$, the decay times obtained from TREC and TRPL traces are essentially the same, as shown in the inset in Fig. 2(a). From Eq. (2), it is also clear that the EC spectrum is proportional to $n_0(\epsilon)$, which reproduce the PL spectrum, but with a negative intensity due to $\delta p_2^0 < \delta p_1^0$.

In Fig. 2(b), the spectral dependence of decay time $\tau(E)$ measured at $T=12$ K are displayed. The decrease in lifetime with the increasing emission energy is a characteristic feature of carrier localizations commonly observed in disordered alloy systems.[20] Similar spectral dependencies of decay time in InN with different electron concentrations have been reported.[3] The localization centers have been attributed to the VB tail states induced by the unintentionally doped n-type impurities.[3,17] The spectral dependence of measured lifetime can be analyzed by[20,21] $\tau(E)=\tau_r/\{1+\exp[(E-E_{me})/E_0]\}$, where τ_r is the radiative lifetime, E_{me} is the mobility edge, and E_0 is a characteristic energy for the density of VB tail states $[\propto \exp(-E/E_0)]$, which can be a measure for the localization energy. As shown by solid lines in Fig. 2(b), good fits are obtained, yielding a radiative lifetime of $\tau_r \sim 0.42$ ns and a localization energy of $E_0 \sim 12$ meV for the as-grown InN. For the annealed InN film, a longer radiative lifetime up to $\tau_r \sim 2.3$ ns and a lower localization energy of $E_0 \sim 8$ meV are obtained due to its lower electron concentration. The measured E_0 are quite close to the depth of VB tail states, which are estimated to be ~ 10 and ~ 6 meV for the as-grown and the annealed samples, respectively, according to the root-mean-square potential fluctuation induced by the randomly distributed ionized impurities.[3,17] In Fig. 2(b), a dip in $\tau(E)$ for the annealed sample is observed but its origin is not clear yet. Since the dip appears near the low-energy shoulder of the PL band, it may arise from transitions involving deeper acceptor states above the VB edge.[16–18]

To further study the influence of the carrier localization on the radiative recombination processes, we have performed temperature-dependent TREC measurements. The measured decay time τ as a function of temperature T for both samples are shown in Fig. 3. The measured $\tau(T)$ consists of both the radiative (τ_r) and the nonradiative (τ_{nr}) components, which can be expressed as $1/\tau = 1/\tau_r + 1/\tau_{nr}$. A standard way to extract τ_r from the measured $\tau(T)$ is to determine the radiative efficiency $\eta(T)=\tau_{nr}/(\tau_{nr}+\tau_r)$ according to the measured temperature-dependent PL intensity, by which the radiative lifetime can be determined using $\tau_r(T)=\tau(T)/\eta(T)$. In Fig. 3, the deduced $\tau_r(T)$ and $\tau_{nr}(T)$ are also displayed. For the as-grown InN film, the deduced τ_r is nearly constant at temperatures below 140 K but above which exhibits a $\tau_r \sim T^{3/2}$ dependence, as expected for bimolecular radiative recombination in direct band-gap semiconductors when the k-selection rule holds.[22,23] The nearly constant τ_r for $T<140$ K indicative of a transition without satisfying the k-selection rule, due to the localization of holes in the VB tail states. For the annealed InN film with lower n_0, the effect of carrier localizations are less pronounced. We found that the temperature dependence restored to $\tau_r \sim T^{3/2}$ for $T>80$ K, indicating that the radiative transition is dominated by the band-to-band recombination process.

Quantitatively, the bimolecular radiative recombination

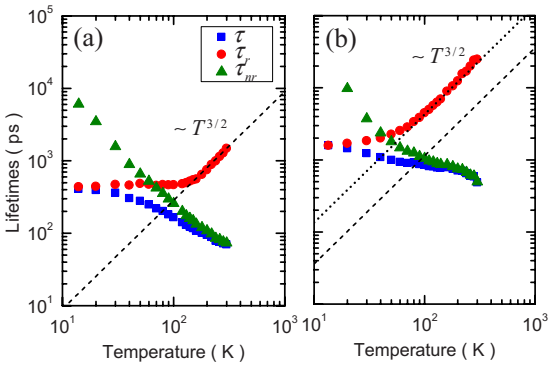

FIG. 3. (Color online) The measured decay time τ as a function of temperature T for (a) the as-grown and (b) the annealed InN films. The deduced radiative $\tau_r(T)$ and nonradiative $\tau_{nr}(T)$ lifetimes are also shown. The dashed lines are calculated $\tau_r(T)$ using n_0 determined from Hall measurements. The dotted line in (b) assumes $n_0=8\times10^{17}$ cm^{-3}.

coefficient B can be determined by the deduced radiative lifetime according to $\tau_r = 1/Bn_0$. By using the expression $B(T)=B_0(300/T)^{3/2}$ and the measured Hall concentration $(1.2\times10^{19}$ cm$^{-3})$ for n_0 to fit the deduced $\tau_r(T)$ in the high-temperature region, we obtain $B_0=5.6\times10^{-11}$ cm^3/s for the as-grown InN film. It should be mentioned that the electron concentration determined by Hall measurements could be higher than the actual concentration in InN bulk due to the presence of surface electron accumulations. Therefore, due to a lack of knowledge of the actual n_0 in InN, the determined values of B can only be considered as a lower limit. For the annealed InN film with a lower electron concentration, the influence of the surface electron accumulation on the Hall measurement would be more significant. In fact, if we use the same B_0 and the measured Hall concentration $(3\times10^{18}$ cm$^{-3})$ for the annealed sample, the predicted radiative lifetimes are much lower than experimental data. Nevertheless, when we modify the electron concentration to $n_0=8\times10^{17}$ cm^{-3} for the annealed sample, a resonant fit to experimental data can be obtained.

According to the Lasher-Stern model,[22,23] the bimolecular coefficient B for the radiative band-to-band recombination is given by

$$B = \frac{(2\pi)^{3/2}\hbar e^2 n_r E_g}{m_0 c^3 [(m_e + m_h)k_B T]^{3/2}} \frac{E_P}{3}, \tag{3}$$

where n_r is the refractive index, E_g is the band-gap energy, E_p is the energy parameter of the momentum matrix element, and m_e (m_h) is the electron (hole) effective mass. By using the following material parameters for InN (Refs. 17 and 24): $E_g=0.7$ eV, $E_p=10$ eV, $n_r=2.9$, $m_e=0.07m_0$, and $m_h=0.3m_0$, where m_0 is the free-electron mass, the calculated B at 300 K is 5.2×10^{-11} cm^3/s, in good agreement with our experimental result. However, the calculated B using Eq. (3) remains uncertain, due to the uncertainty of used material parameters, particularly the value of hole effective mass m_h. We would also like to point out that Eq. (3) is derived based on transitions between nondegenerate carriers near the edges of parabolic bands. It would be less accurate for transitions

involving the degenerate electrons in the conduction band with a strong nonparabolicity in such highly unintentionally doped InN films.

In summary, recombination dynamics in degenerate InN with different electron concentrations have been investigated by means of time-resolved excitation-correlation spectroscopy. The PL decay times are determined beyond the spectral response and temporal resolution limits of conventional photon-counting detectors. Spectral and temperature dependence of decay times reveal that the hole localization in the VB tails play a decisive role in the recombination process. At low temperatures, the radiative lifetime τ_r is insensitive to temperature and significantly longer than that predicted for the radiative band-to-band recombination, indicating that the PL emission from InN is dominated by the free-to-bound recombination process without k conservation. Above a certain temperature determined by the carrier concentration, the temperature dependence restored to $\tau_r \sim T^{3/2}$, as expected for the radiative band-to-band transitions when the k-selection rule holds. We determine a lower limit for the bimolecular recombination coefficient B in InN at 300 K as 5.6×10^{-11} cm^3/s.

This work was supported in part by the program of MOE-ATU and the National Science Council of Taiwan under Grant No. NSC-97-2112-M-009-015-MY2.

*whchang@mail.nctu.edu.tw

[1] J. Wu, J. Appl. Phys. **106**, 011101 (2009).
[2] R. Intartaglia, B. Maleyre, S. Ruffenach, O. Briot, T. Taliercio, and B. Gil, Appl. Phys. Lett. **86**, 142104 (2005).
[3] G. W. Shu, P. F. Wu, M. H. Lo, J. L. Shen, T. Y. Lin, H. J. Chang, Y. F. Chen, C. F. Shih, C. A. Chang, and N. C. Chen, Appl. Phys. Lett. **89**, 131913 (2006).
[4] B. Liu, R. Zhang, Z. L. Xie, X. Q. Xiu, Z. X. Bi, S. L. Gu, Y. Shi, Y. D. Zheng, L. J. Hu, Y. H. Chen, and Z. G. Wang, Appl. Phys. Lett. **87**, 176101 (2005).
[5] D.-J. Jang, G.-T. Lin, C.-L. Wu, C. L. Hsiao, and L. W. Tu, Appl. Phys. Lett. **91**, 092108 (2007).
[6] D.-J. Jang, G.-T. Lin, C.-L. Hsiao, L. W. Tu, and M.-E. Lee, Appl. Phys. Lett. **92**, 042101 (2008).
[7] F. Chen, A. N. Cartwright, H. Lu, and W. J. Schaff, Appl. Phys. Lett. **83**, 4984 (2003).
[8] F. Chen, A. N. Cartwright, H. Lu, and W. J. Schaff, Phys. Status Solidi A **202**, 768 (2005).
[9] D. Rosen, A. G. Doukas, Y. Budansky, A. Katz, and R. R. Alfano, Appl. Phys. Lett. **39**, 935 (1981).
[10] A. Olsson, D. J. Erskine, Z. Y. Xu, A. Schremer, and C. L. Tang, Appl. Phys. Lett. **41**, 659 (1982).
[11] M. Jorgensen and J. M. Hvan, Appl. Phys. Lett. **43**, 460 (1983).
[12] M. B. Johnson, T. C. McGill, and A. T. Hunter, J. Appl. Phys. **63**, 2077 (1988).
[13] J. L. A. Chilla, O. Buccafusca, and J. J. Rocca, Phys. Rev. B **48**, 14347 (1993).
[14] W. C. Ke, C. P. Fu, C. Y. Chen, L. Lee, C. S. Ku, W. C. Chou, W. H. Chang, M. C. Lee, W. K. Chen, W. J. Lin, and Y. C. Cheng, Appl. Phys. Lett. **88**, 191913 (2006).
[15] W. C. Ke, L. Lee, C. Y. Chen, W. C. Tsai, W.-H. Chang, W. C. Chou, M. C. Lee, W. K. Chen, W. J. Lin, and Y. C. Cheng, Appl. Phys. Lett. **89**, 263117 (2006).
[16] W.-H. Chang, W.-C. Ke, S.-H. Yu, L. Lee, C.-Y. Chen, W.-C. Tsai, H. Lin, W.-C. Chou, M.-C. Lee, and W.-K. Chen, J. Appl. Phys. **103**, 104306 (2008).
[17] B. Arnaudov, T. Paskova, P. P. Paskov, B. Magnusson, E. Valcheva, B. Monemar, H. Lu, W. J. Schaff, H. Amano, and I. Akasaki, Phys. Rev. B **69**, 115216 (2004).
[18] A. A. Klochikhin, V. Yu. Davydov, V. V. Emtsev, A. V. Sakharov, V. A. Kapitonov, B. A. Andreev, Hai Lu, and William J. Schaff, Phys. Rev. B **71**, 195207 (2005).
[19] The photogenerated carrier density can be estimated by $\delta n = \alpha P_{ex}/(eAh\nu R_{\mathrm{rep}})$, where α is the absorption coefficient, P_{ex} is the excitation power, e is the electron charge, A is the excitation area, $h\nu$ is the photon energy, and $R_{\mathrm{rep}}=80$ MHz is the laser repetition rate. For $P_{ex}=1$ mW, $\alpha=7\times10^4$ cm^{-1} for InN at $\lambda=780$ nm, and a laser spot radius of ~ 30 μm, we estimated $\delta n \sim 1.2\times10^{17}$ cm^{-3}.
[20] M. Strassburg, M. Dworzak, H. Born, R. Heitz, A. Hoffmann, M. Barteis, K. Lischka, D. Schikora, and J. Christen, Appl. Phys. Lett. **80**, 473 (2002).
[21] C. Gourdon and P. Lavallard, Phys. Status Solidi B **153**, 641 (1989).
[22] G. Lasher and F. Stern, Phys. Rev. **133**, A553 (1964).
[23] H. T. Grahn, *Introduction to Semiconductor Physics* (World Scientific, Singapore, 1999).
[24] J. Wu, W. Walukiewicz, W. Shan, K. M. Yu, J. W. Ager III, E. E. Haller, H. Lu, and W. J. Schaff, Phys. Rev. B **66**, 201403(R) (2002).